J Nanopart Res (2020) 22:48
https://doi.org/10.1007/s11051-020-4770-4

RESEARCH PAPER

Magnetic nanoparticle recovery device (MagNERD) enables application of iron oxide nanoparticles for water treatment

Camilah D. Powell · Ariel J. Atkinson · Yizhao Ma · Mariana Marcos-Hernandez · Dino Villagran · Paul Westerhoff · Michael S. Wong

Received: 21 October 2019 / Accepted: 30 January 2020

Abstract An optimized permanent magnetic nanoparticle recovery device (i.e., the MagNERD) was developed and operated to separate, capture, and reuse superparamagnetic Fe_3O_4 from treated water in-line under continuous flow conditions. Experimental data and computational modeling demonstrate how the MagNERD's efficiency to recover nanoparticles depends upon reactor configuration, including the integration of stainless-steel wool around permanent magnets, hydraulic flow conditions, and magnetic NP uptake. The MagNERD efficiently removes Fe_3O_4 in the form of a nanopowder, up to > 95% at high concentrations (500 ppm), under scalable and process-relevant flow rates (1 L/min through a 1.11-L MagNERD reactor), and in varying water matrices (e.g., ultrapure water, brackish water). The captured nanoparticles were recoverable from the device using a simple hydraulic backwashing protocol. Additionally, the MagNERD

Camilah D. Powell and Ariel J. Atkinson contributed equally to this work.

This article is part of the topical collection: *Nanotechnology Convergence in Africa*

Guest Editors: Mamadou Diallo, Abdessattar Abdelkefi, and Bhekie Mamba

Electronic supplementary material The online version of this article (https://doi.org/10.1007/s11051-020-4770-4) contains supplementary material, which is available to authorized users.

C. D. Powell · M. S. Wong
Chemical and Biomolecular Engineering, Rice University, Houston, TX, USA

C. D. Powell · A. J. Atkinson · Y. Ma · M. Marcos-Hernandez · D. Villagran · P. Westerhoff · M. S. Wong
Nanosystems Engineering Research Center for Nanotechnology-Enabled Water Treatment, Houston, USA

M. S. Wong
Civil and Environmental Engineering, Rice University, Houston, TX, USA

M. S. Wong (✉)
Chemistry, Rice University, Houston, TX, USA

M. S. Wong (✉)
Material Science and NanoEngineering, Rice University, Houston, TX, USA
e-mail: mswong@rice.edu

M. Marcos-Hernandez · D. Villagran
Department of Chemistry and Biochemistry, University of Texas at El Paso, El Paso, TX, USA

A. J. Atkinson · Y. Ma · P. Westerhoff
School of Sustainable Engineering and The Built Environment, Arizona State University, Tempe, AZ, USA

Published online: 12 February 2020

removed ≥ 94% of arsenic-bound Fe_3O_4, after contacting As-containing simulated drinking water with the nanopowder. The MagNERD emerges as an efficient, versatile, and robust system that will enable the use of magnetic nanoparticles in larger scale water treatment applications.

Keywords Environmental nanotechnology · Adsorption · Nano-magnetism · Arsenic

Introduction

Functionalized superparamagnetic nanoparticles—or nanosorbents—can be used to remove contaminants from water enabling various applications (Gutierrez et al. 2017). However, it is essential to integrate a system within each application that can remove all magnetic nanosorbents after contaminant sorption. Removing the nanosorbents is intended to ensure nanoparticle concentrations and/or dissolved species do not exceed primary or secondary regulatory limits for water (e.g., total iron < 300 ppb for potable water). In literature, most studies using magnetic nanoparticles are performed at the bench scale and utilize handheld magnets for magnetic capture. Unfortunately, handheld magnetic separation techniques become infeasible when treating continuous flows or large volumes of water. Additionally, these studies rarely address magnetic capture using realistic water matrices or conditions nor the extent of magnetic nanoparticle removal. While advances have been recognized in surface modification and synthesis techniques of superparamagnetic nanoparticles for environmental applications (Reza and Mirrahimi 2010), relatively few reports (Moeser et al. 2004) quantify nanoparticle capture or recovery or include details on relevant nanoparticle separation methods.

High gradient magnetic separation (HGMS) can be a viable candidate to remove magnetic nanomaterials deployed in large-scale waters (Moeser et al. 2004; Yavuz et al. 2010; Qu et al. 2013; Gómez-Pastora et al. 2014; Westerhoff et al. 2016). HGMS systems use strong magnets (i.e., permanent or electromagnetic) and magnetically susceptible wires to capture micron-sized magnetic particles (Oberteuffer 1973; Gerber 1978; Zborowski et al. 1999; Hatch and Stelter 2001). As a green separation technology that requires less operational energy than conventional separation methods (i.e., membrane separation, settling, etc.), HGMS has garnered attention within the water purification and nanotechnology-assisted water treatment fields. While robust and not limited by variations in pH or ionic concentration (Ambashta and Sillanpää 2010; Mariani et al. 2010; Toh et al. 2012; Gómez-Pastora et al. 2014; Rossi et al. 2014), its optimization and use with magnetic nanoparticles in water treatment is limited (Gómez-Pastora et al. 2014; Rossi et al. 2014). The extent and quality of magnetic capture by HGMS depends on a variety of forces and interactions—magnetic, viscous, inertial forces, gravity, friction, and interparticle interactions—acting on each magnetic particle, and all of which must be properly optimized with respect to each other for effective magnetic capture (Oberteuffer 1973, 1974; Gómez-Pastora et al. 2014). For example, capture efficiency and the ability to recover the nanoparticles from the HGMS system is heavily size dependent, with capture efficiency increasing with increasing particle size and recovery decreasing with increasing particle size (Moeser et al. 2004; Yavuz et al. 2006).

To enable the use of HGMS systems as part of a water treatment process at pilot- and full-scale, a proof-of-concept demonstration needs to be performed. Additionally, the HGMS system must (i) effectively capture nanosized magnetic materials to below application specific limits (e.g., the EPA secondary maximum contaminant level (SMCL) for iron in drinking water is < 0.3 mg-Fe/L) to move the technology forward and (ii) potentially enable recovery of nanoparticles for subsequent reuse in the water purification system. Related non-nanotechnologies are already employed in the water industry (Ringler et al. 2018; Zhu et al. 2019). For example, millimeter-size magnetic ion exchange resin particles is an alternative to chemical coagulants (e.g., alum, ferric chloride) to remove natural organic matter. After use and separation, the resin is regenerated using a strong base and then reused. Processes to do the same with superparamagnetic nanoparticles have yet to be demonstrated in continuous flow for water treatment.

In this manuscript, we develop a continuous flow nanoparticle separation and capture process using a magnetic nanoparticle removal device (termed "MagNERD"). We performed process optimization and the effects of operational parameters (i.e., flowrate, amount of exposed magnetized surface area, and system orientation); modeled fluid flow inside of the MagNERD using computational fluid dynamics; demonstrated the ability of the MagNERD to remove magnetically nanosized adsorbents with sorbed

contaminants from flowing water; and explored the MagNERD's feasibility to recover, clean, and reuse the magnetic particles (Fig. 1).

Materials and methods

Magnetic capture unit flow simulations

Simulating fluid flow with computational fluid mechanics simulation software (COMSOL) was carried out to understand the effect of unit design and stainless-steel wool on the potential ability to remove magnetic nanoparticles from flowing water. The MagNERD unit was modeled as a packed-bed reactor. Fluid streamlines for the reactor with and without stainless-steel wool were generated by solving the continuity equation (i.e., characterizing the conservation of mass), the Navier-Stokes equation (i.e., characterizing the conservation of momentum), and the Brinkman equation, respectively (Eqs. S1–S11) (Deen 2011). The Brinkman equation is a modification of the Navier-Stokes equation and accounts for the viscous forces of the fluid passing through the pores of the stainless-steel wool matrix by including the porosity (0.998) and permeability of a porous matrix ($0.0305\ m^2$). Other assumptions and model parameters are provided in the electronic supplemental material.

Materials and characterization

Magnetite iron oxide nanopowder (Fe_3O_4) was purchased from US Research Nanomaterials, Inc. with a metal basis purity of 99.6% and a specific surface area of 82 m^2/g as reported by the manufacturer. The nanopowder (NP) is comprised of aggregated nanoparticles with sizes ranging from 15 to 20 nm as reported by the manufacture.

Simulated brackish water and arsenic-spiked simulated drinking water were synthesized with the following ACS-grade chemicals purchased from Sigma Aldrich: $CaCl_2$-H_2O, $MgSO_4 \cdot 7H_2O$, NaCl, $Na_2SO_4 \cdot 10H_2O$, $NaHCO_3$, NaOH, and HCl, $Na_2SiO_2 \cdot 9H_2O$, $NaNO_3$, $NaH_2PO \cdot H_2O$, and NaF (fluoride standard solution from Ricca Chemical). Sodium arsenate (Na_3AsO_4 in the form of an Atomic Adsorption Spectroscopy Arsenic Standard from Sigma Aldrich; 1000 mg/L As in 2% nitric acid prepared with high purity As_2O_3, HNO_3, NaOH, and H_2O) was used.

Magnetic characterization was conducted with a superconducting quantum interference device (SQUID) completed with a MPMS XL (Quantum Design Inc.).

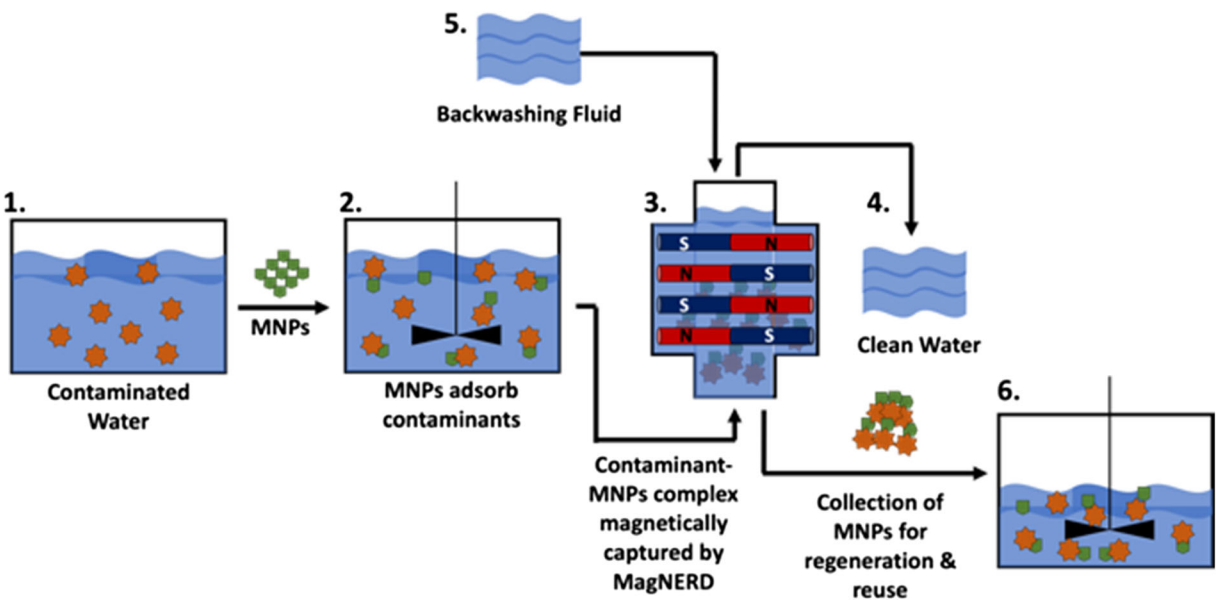

Fig. 1 Magnetic capture/removal scheme of contaminants from water using the magnetic 3D reactor. 1. Contaminated water is introduced to magnetic nanopowders (MNPs). 2. The contaminants within the water adsorb onto the MNPs upon mixing. 3. The contaminant-MNPs complex is magnetically separated from the water using a permanent magnet mounted within a reactor. 5. A small portion of water is passed through the outlet of the MagNERD to flush out the contaminant-MNPs complexes. 6. The flushed contaminant-MNPs complexes are collected for future regeneration and reuse completing the MNP recovery process

Hysteresis curves were collected for Fe_3O_4 and arsenic bound Fe_3O_4 NPs. For each measurement, the material was weighed, wrapped in Teflon tape, and measured from − 10 to 10 kOe at a constant temperature (300 K).

Synthesis of simulated brackish water and simulated drinking water

Simulated brackish water was prepared using the following salt concentrations: $CaCl_2{\cdot}H_2O$ (3925 mg/L), $MgSO_4{\cdot}7H_2O$ (2637 mg/L), NaCl (2397 mg/L), $Na_2SO_4{\cdot}10H_2O$ (1381 mg/L), and $NaHCO_3$ (1280 mg/L). The solution pH was adjusted to 7.5 using HCl (1.0 M). The resulting ionic strength and total dissolved solids (TDS) values were ~ 190 mM and ~ 8429 mg/L, respectively.

Simulated drinking water was prepared in accordance with the NSF challenge water (National Science Foundation 2013) by using the following salt concentrations: $NaHCO_3$ (252 mg/L), $CaCl_2{\cdot}H_2O$ (147 mg/L), $MgSO_4{\cdot}7H_2O$ (124 mg/L), $Na_2SiO_2{\cdot}9H_2O$ (95 mg/L), $NaNO_3$ (12 mg/L), NaF (2.2 mg/L), and $NaH_2PO_4{\cdot}H_2O$ (0.18 mg/L). The solution was adjusted to pH 7.5 using HCl (1.0 M), and the resulting ionic strength and total dissolved solids (TDS) values were ~ 8.5 mM and ~ 478 mg/L, respectively.

Preparation of the NP slurries

Concentrated NP slurries were made by mixing 9 g of NP (e.g., Fe_3O_4 with 1 L of test water—DI or simulated brackish water). Concentrated NP solutions were dispersed with a probe sonicator for 25 min at a pulse rate of 282 s and amplitude of 45%. An ice bath was used to surround the beaker during the sonication process to prevent excessive heating. The concentrated NP solutions were then diluted to 18 L to give a final NP concentration of 500 ppm. Dilution occurred under constant mixing to ensure a uniform dispersion of NP.

Magnetic capture system (MagNERD)

The MagNERD unit was purchased from Eriez Inc. (a stainless-steel Super B-2 Model Trap) and consisted of five parts: (1) the main enclosure, (2) five columns of neodymium magnetic fingers, (3) a stainless-steel protective sleeve for the magnetic fingers, (4) a seal ring, and (5) a fine mesh filter screen. The entire apparatus (Fig. 2) has a maximum fluid volume of 1.11 L. For all experiments, the five magnetic fingers were kept inside of the protective sleeve to preserve their integrity. The sleeved fingers were placed inside of the main enclosure. The seal ring was used to seal the sleeved fingers and the main enclosure together and prevent leaks. In select experiments, stainless-steel wool (SSW; wire diameter of 50 μm, grade 434 stainless steel) was wrapped around each sleeved finger throughout the full extent of the reactor. The total amount of SSW used within the unit was ~ 20 g. The entire magnetic recovery system and reactor setup are shown in Fig. 2 and Fig. S1, respectively.

Magnetic NP capture and recovery using MagNERD

Magnetic NP capture

Unless otherwise specified, the MagNERD was fitted with ~ 20 g of SSW for all magnetic capture experiments. Each experiment was carried out with 18 L of 500 ppm NP suspensions subjected to constant stirring. NP suspensions were passed through the MagNERD with a peristaltic pump at one of two flowrates: 0.3 L/min or 1 L/min. The MagNERD was either vertically (water flowing upward) or horizontally aligned as shown in Fig. 3.

Every 3 min, 25-mL samples of the effluent were collected for analysis until the entire effluent was captured. Effluent samples were analyzed with UV-vis spectroscopy (Shimazdu UV-2450 UV-Spectrophotometer) at 365 nm, the wavelength at which the Fe_3O_4 NP showed maximum absorbance. Calibration curves were generated to quantify NP concentrations at mg/L (Fig. S2). The capture efficiency and mass loading of the MagNERD were calculated using Eqs. 1 and 2 as a function of the NP concentration in the influent (C_{sol}) and effluent (C_{eff}) solutions.

$$\text{NP Capture Efficiency}(\%) = \frac{C_{\text{Soln}} - C_{\text{Eff}}}{C_{\text{Soln}}} \times 100\% \quad (1)$$

$$\text{Cumulative NP Uptake (mg)} = C_{\text{Soln}}\left(\frac{\text{mg}}{\text{L}}\right) \times \text{Flow Rate}\left(\frac{\text{L}}{\text{min}}\right) \times \text{Time(min)} \quad (2)$$

Magnetic NP recovery

To recover the NPs once magnetically captured, the MagNERD was backwashed. After the NP suspension

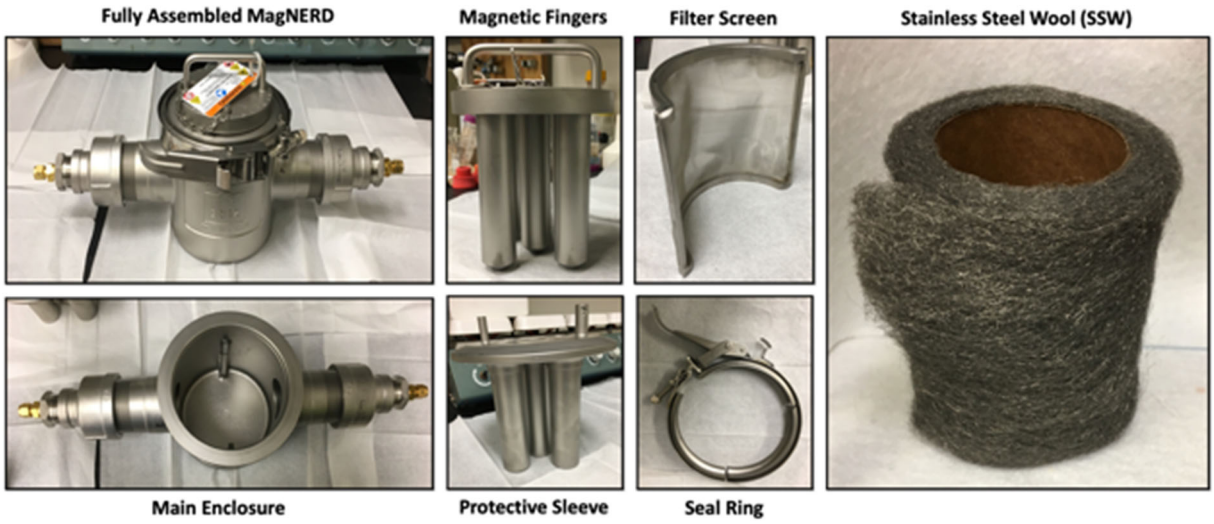

Fig. 2 The MagNERD apparatus with components displayed and labeled

passed through the MagNERD, the permanent magnetic fingers were removed from their sleeve and set aside. The MagNERD was flushed with 3.4 L of DI water in the opposite flow direction as the initial magnetic capturing experiments. The flushed NP suspension was captured, dried (105 °C for 24 h) and weighed. Recovery efficiency was calculated using Eq. 3.

$$\text{NP Recovery Efficiency}(\%) = \frac{\text{Weight of recovered dry NP}}{\text{Weight of NP initially added}} \times 100\% \quad (3)$$

Arsenic removal from simulated drinking water

The ability of the magnetic particles to adsorb arsenic in batch experiments and then to be removed from flowing water by the MagNERD was evaluated using a simulated drinking water matrix containing arsenic (100 ppb-AsO_4). Fe_3O_4 (0.5 g/L)—the adsorbent media—was added to the 12 L of arsenic-spiked–simulated drinking water and stored within LDPE bottles. Adsorption experiments were conducted at 25 °C. Samples were continuously agitated for 72 h to ensure equilibrium. Liquid aliquots (10 mL) were filtered with a 0.2-μm Nylon syringe filter and collected for analysis at the end of the adsorption period. The equilibrium water-phase concentration of arsenic was quantified using a Thermo Scientific X-Series II inductively coupled plasma mass spectrometer (ICP-MS).

At the end of the adsorption period, the 12-L suspension was continuously mixed with a mechanical stirrer and passed through the MagNERD at a flowrate of 1 L/min. During magnetic capture, the effluent was collected, and 50-mL samples were taken every 3 min. The concentration of magnetic absorbent in the effluent was quantified by absorbance at $\lambda = 365$ nm (SI Fig. S2). Capture efficiency was calculated with Eq. 1.

Results and discussion

Magnetic capture unit flow simulations

Streamline profiles of the COMSOL flow simulations are displayed in Fig. 4. In the horizontal configuration, the MagNERD volume is filled with the feed suspension with eddy currents (e.g., back mixing) emerging behind each magnetic finger for high flowrates (i.e., 1 L/min; Fig. 4a, b). The SSW had a negligible effect on fluid flow inside of the MagNERD and yields negligible pressure drop (Fig. 4a, b).

For the comparative vertical upward flow scheme, the entire MagNERD volume is filled with fluid regardless of flowrate with back mixing emerging at higher flowrates behind the magnetic fingers closest to the inlet (1 L/min; Fig. 4c, d). The model suggests more back mixing occurs in the vertical upward high flow rate regime, evident by a higher concentration of contours behind the right inlet magnetic finger, due to gravity forces. This suggests that the feed suspension will have

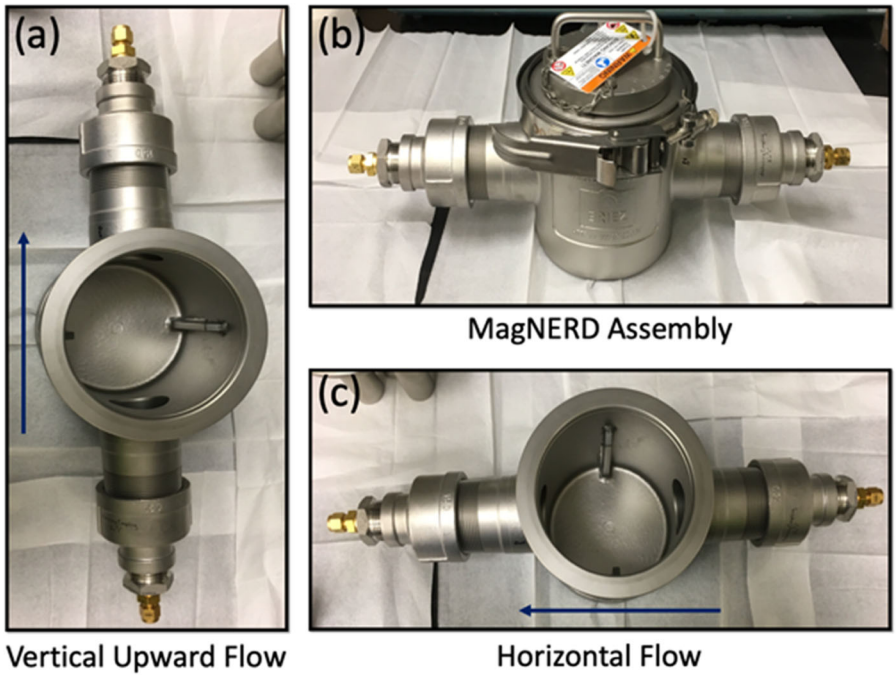

Fig. 3 Flow orientations used for the MagNERD: **a** vertical upward flow, **b** entire MagNERD assembly, **c** horizontal flow

more interactions with the magnetic fingers at the inlet and potentially capture more magnetic NP at the front of the MagNERD than the horizontal flow scheme.

MagNERD optimization and capture efficiency

Horizontal versus vertical configuration

To determine the optimal flow configuration of the MagNERD, the amount of NP captured at the target flowrate (1 L/min) was compared for the vertical upward flow scheme and the horizontal flow scheme (Fig. 3). The upward flow regime had a capture efficiency > 85% (Fig. 5a; blue circles). Comparatively, the horizontal flow regime had a capture efficiency between 65 and 80% (Fig. 5a; orange diamonds) and a capture efficiency of ~ 12% without magnetic components present. For both the horizontal and vertical flow regimes, most of the magnetic NP was captured at the front of the reactor as predicted with COMSOL modeling (Figs. 4 and 5b, c). Additionally, the higher capture efficiency of the vertical upward flow configuration can be attributed to the contact availability of magnetized surface area at the inlet of the reactor. For the vertical upward flow scheme, the NP suspension contacted the full height of the magnetic fingers and magnetized SSW within the reactor (Fig. 5c). This was not the case for the horizontal flow configuration; NP contact with the magnetized surfaces was limited to half the total height of the magnetic fingers and SSW (Fig. 5b). In subsequent experiments, the vertical upward flow configuration was chosen.

Flowrate

Figure 6a shows that under all testing conditions, the MagNERD removed NPs (94–97% removal) better than the handheld magnet control (80–85% removal). The effect of flowrate on NP capture was evaluated using two flow rates: a low flow rate relevant to bench scale operations (0.3 L/min) and a high flow rate relevant to pilot or proof-of-concept scale operations (1 L/min). The low flowrate had greater capture efficiency (97%) than the high flowrate (95%; Fig. 6a). Presumably, lower flowrates increase magnetic capture due to increased contact time between the NP suspension and the magnetized surfaces.

Although the MagNERD achieved a 95% NP capture efficiency, the effluent iron concentration (~ 25 mg/L) exceeded the USEPA drinking water SMCL of 0.3 mg/L for iron. For non-potable applications or disposal (e.g., industrial wastewater

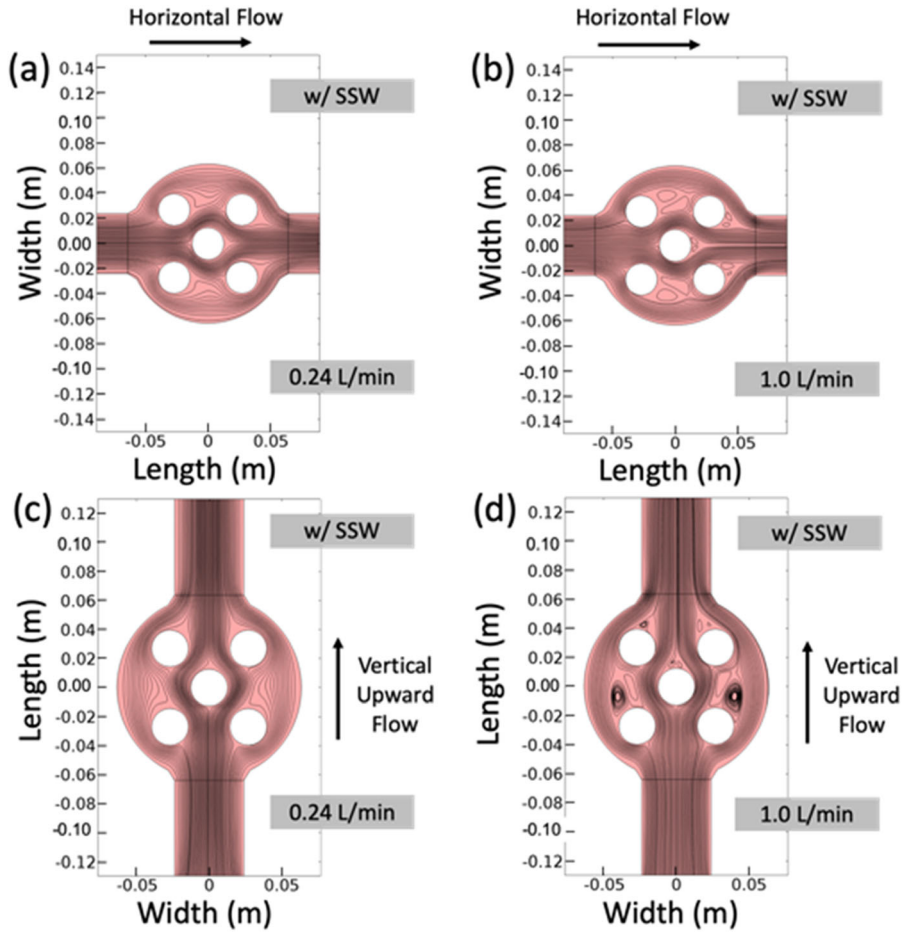

Fig. 4 Fluid streamlines in the magnetic 3D reactor viewed from the top: **a** MagNERD in horizontal flow with and without SSW at 0.24 L/min, **b** MagNERD in horizontal flow with and without SSW at 1.0 L/min, **c** MagNERD in vertical upward flow with and without SSW at 0.24 L/min, **d** MagNERD in vertical flow with & without SSW at 1.0 L/min. The velocity profile changes with increasing flow rate. The magnetic fingers are depicted as white circles

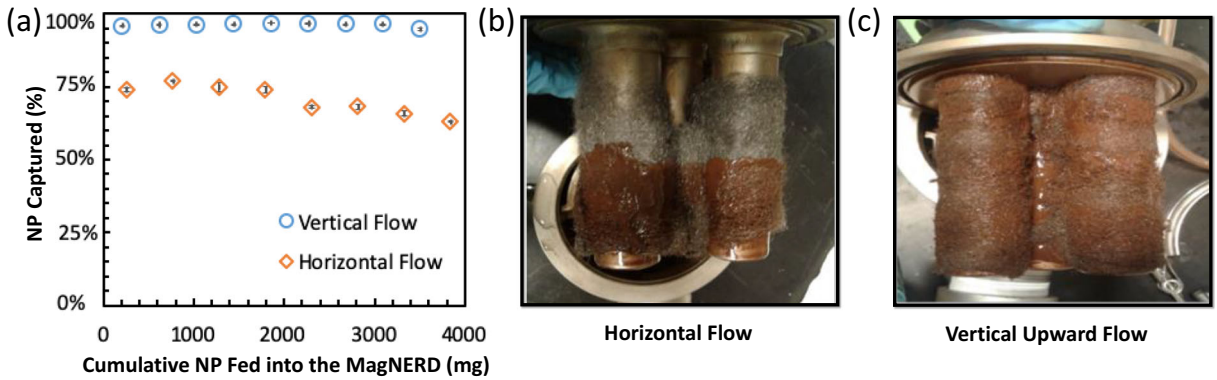

Fig. 5 Effect of reactor configuration on **a** Fe_3O_4 NP capture efficiency with horizontal flow (orange diamonds) versus vertical upward flow (blue circles) and location of NP capture on the magnetized SSW/magnetic fingers when operated in **b** horizontal flow configuration versus **c** vertical upward flow configuration. MagNERD was operated with SSW, 500 ppm Fe_3O_4 NP in DI water, and at 1 L/min

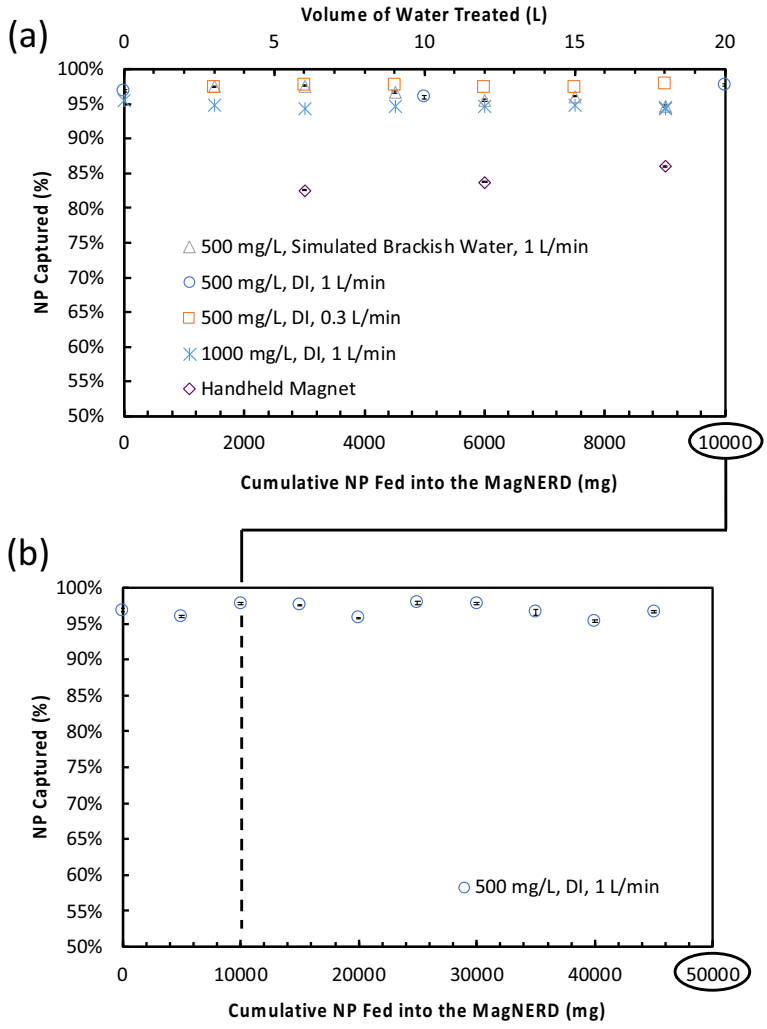

Fig. 6 **a** Fe_3O_4 NP removal efficiency for the MagNERD: (green triangles) 500 mg-Fe_3O_4/L in simulated brackish water at a flowrate of 1.0 L/min; (blue circles) 500 mg/L in DI water at 1.0 L/min; (orange squares) 500 mg/L in DI water at 0.3 L/min; and (light blue asterisks) 1000 mg/L in DI water at 1.0 L/min. (purple diamonds) Fe_3O_4 NP removal efficiency for a handheld magnet using 500 mg/L of Fe_3O_4 NP in DI water. **b** Fe_3O_4 NP removal efficiency for the MagNERD containing SSW up to 90 L of water (500 mg/L in DI water at 1.0 L/min)

treatment) the presence of iron in the effluent is likely a lower priority than for drinking water. Based upon a 95% NP removal, the initial Fe_3O_4 NP concentrations should be limited to ≤ 6 mg/L to meet the drinking water standards. Alternatively, the MagNERD can undergo a multi-pass configuration—where the effluent passes through the MagNERD multiple times—to increase the amount of magnetic NP captured (e.g., from ~60 to 70% upon the 2nd pass, Fig. S3a) and decrease the amount of Fe_3O_4 NP in the resulting effluent (e.g., effluent Fe_3O_4 NP concentration decreases ~ 78% from the 1st pass to the 2nd pass; Fig. S3b). These results indicate that if the magnetic surface area of MagNERD was doubled, the removal of NP could be increased by an order of magnitude, i.e., from 95% removal and effluent concentration of 25 mg/L in one pass to 99.8% removal and effluent concentration 1 mg/L in two passes or with doubling the magnetic surface area.

Influent NP concentration and mass loading

The effect of NP concentration on NP capture was also evaluated. Figure 6a shows that the initial NP concentration did not substantially affect capture efficiency. The MagNERD successfully captured ≥ 94% of the Fe_3O_4 NP for influent NP concentrations of 500 ppm (blue circles) and 1000 ppm (light blue asterisks). Therefore, we believed the system was mass loading dependent rather than concentration dependent. However, we were not able to exceed a mass loading that decreased the removal efficiency of NP potentially because of the large amount of magnetized surface area within the

reactor (e.g., the SSW; 0.486 cm^2/g-SSW). Even as the NP mass loaded into the system exceeded 50 g, removal efficiencies remained above 94% (Fig. 6b).

Water matrix

The water treatment application of magnetic NPs could range from the removal of ionic species in ultrapure water to industrial wastewater for drinking water purposes to non-potable reuse or even to meet disposal requirements. Therefore, to encapsulate this range of influent waters, we compared the capture of magnetic NPs in deionized water (< 1.6 mM TDS) and simulated brackish water (190 mM TDS). No matter the water matrix, the MagNERD consistently maintained a NP capture efficiency > 95% (Fig. 6a).

Recovery of NP from MagNERD for reuse

Backwashing experiments were conducted to determine the MagNERD's ability and efficiency to recover NP for reuse. For experiments with or without SSW, the MagNERD was flushed with ~ 4 L (e.g., 20% of treated water) of the initially treated water (MagNERD effluent). The majority of NP recovered were in the first 500 mL (e.g., 2.5% of treated volume). The recovery efficiency for Fe_3O_4 NP in the absence of steel wool (~ 75%, some NP remained on the magnetic fingers) is nearly double the recovery efficiency for Fe_3O_4 NP in the presence of steel wool (~ 44%). The reduced recovery of NP from the MagNERD with SSW present is likely due to (i) increased residual magnetization with SSW, (ii) the formation of large Fe_3O_4 nanoparticle aggregates which become stuck within the mesh-like structure of the SSW (Yavuz et al. 2006), and (iii) the inability of the fluid shear forces to remove the nanoparticle aggregates from the SSW pores. With and without SSW, the NP that remained in the system was visibly left on the previously magnetized surfaces (i.e., fingers and SSW). Depending on the requirements of the application, the SSW may not be desirable to use due to inability to clean out the MagNERD for subsequent use and/or the limited ability to recover the NP. If much more than 4 g is loaded into MagNERD, the SSW may enable more capture as opposed to the magnetic fingers alone, though this is speculation and was not directly observed. If this hypothesis were true and the capture of a high amount of NP was needed—and the ability to recover NP for reuse was not a priority—then the SSW could just be replaced after the maximum loading was exceeded and NP capture efficiency decreased.

Demonstrating arsenic removal with the MagNERD

A proof-of-concept experiment was performed to demonstrate the use of the MagNERD to remove adsorbents adsorbed with a target pollutant (arsenic) from realistic waters under a realistic operational scenario. Simulated drinking water (12 L) containing arsenate (100 ppb-AsO_4) was first contacted with Fe_3O_4 NP (0.5 g/L), and then the suspension was pumped through the MagNERD at 1 L/min. On average, 0.5 g/L of Fe_3O_4 removed ~ 35 μg/L As from the simulated drinking water (i.e., 0.976 μg-As/m^2-Fe_3O_4), and ≥ 95% of the resulting As-Fe_3O_4 NP was removed by the MagNERD (Fig. 7a). The water quality improved, with the treated water containing ~ 60 μg-As/L and ≤ 20 mg-Fe_3O_4/L (compared with the initial solution of ~ 100 μg-As/L and ~ 360 mg-Fe_3O_4/L).

The Fe_3O_4 NP was superparamagnetic-like, as verified by its low coercivity (Hc), magnetic remanence (Mr), and extent of ferromagnetism (Mr/Ms) (Fig. S4, Table S1) (Mahmoudi et al. 2011; Qu et al. 2013). Given its substantial magnetic saturation (~ 50 emu/g), the Fe_3O_4 NP proved to have a strong magnetic attraction to the magnetized components in the MagNERD as evident by the large capture efficiencies achieved by the MagNERD (Fig. 7a, blue triangles) (Moeser et al. 2004; Yavuz et al. 2006; Rossi et al. 2014). The weight of the amount of sorbed arsenic species onto the surface of the Fe_3O_4 NP was found to be 80 μg-As per g-Fe_3O_4.

The addition of the sorbed non-magnetic arsenic atoms (Kikoin et al. 2015) on the surface of the Fe_3O_4 NP reduced its magnetic saturation by approx. 38% (i.e., M_s for Fe_3O_4 ~ 50 emu/g whereas M_s for As-Fe_3O_4 ~ 31 emu/g; Fig. 7b). The additional mass of the adsorbed arsenic (~ 0.01 wt% of the As-Fe_3O_4 complex) is too small to account for the loss of magnetic saturation. This loss is attributable to surface spin disorder caused by the interactions between the non-magnetic adsorbed arsenic atoms and the magnetic Fe_3O_4 (Larumbe et al. 2012; Tang et al. 2014; Veligatla et al. 2015). However, in spite of the depression,

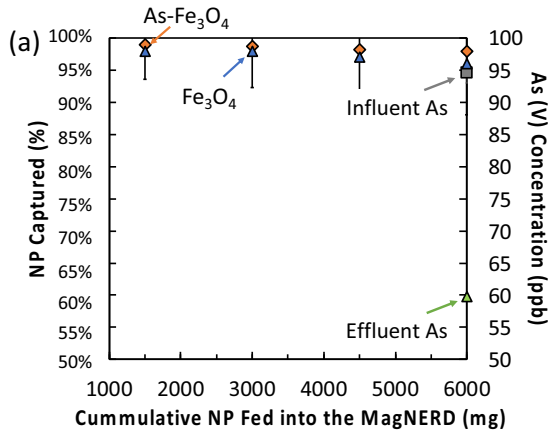

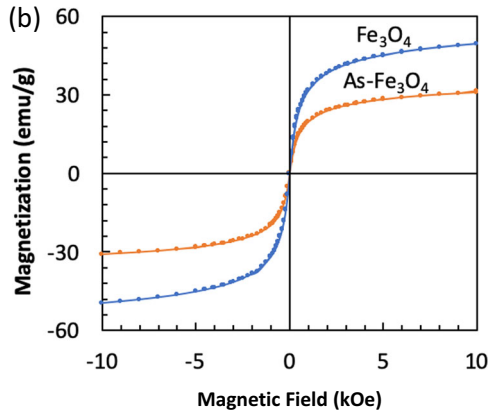

Fig. 7 **a** MagNERD capture efficiency for As-Fe_3O_4 (orange diamonds) and Fe_3O_4 (blue triangles) in simulated drinking water at 1 L/min. Arsenic concentration of effluent (green), compared to influent concentration (gray square). **b** M vs. H curves for the Fe_3O_4 nanopowder before (blue) and after arsenic adsorption (orange curve)

the magnetic saturation of the As-Fe_3O_4 was still large enough to produce MagNERD capture efficiencies above 90% (Fig. 7a, orange diamonds). Such results successfully demonstrate the MagNERD's ability to remove As-Fe_3O_4 from water treatment schemes under flow conditions.

Conclusions

Because of the inability to separate nanoparticles from flowing water, hesitation has surrounded the large-scale use of beneficial nanoadsorbents for water remediation. To alleviate such concerns, high gradient magnetic separation (HGMS) is a promising green separation technology that can facilitate the effective removal of nanoabsorbents from water once optimized. In this work, we developed a cost effective, large scale, HGMS system (MagNERD) for remote, real world working conditions and describe its optimization. From modeling, the optimal flow configuration for effective capture efficiency was successfully predicted. Also, further testing proved SSW to be beneficial for exceptionally large NP mass loadings (i.e., 50 g) maintaining capture efficiencies > 94%. Lastly, given its ability to remove ≥ 94% of As-Fe_3O_4 from simulated drinking water after arsenic treatment, the MagNERD can be envisaged as an excellent technology to be integrated into real world water treatment schemes. As found, the MagNERD can effectively capture (> 94%) and recover (> 80%) magnetic nanoadsorbents from complex water matrices under process relevant flow conditions encouraging the safe use of nanomaterials for large-scale water treatment systems.

Acknowledgements The authors wish to acknowledge the staff and facilities of the Shared Equipment Authority at Rice University.

Funding information This work was funded by the National Science Foundation (EEC-1449500) Nanosystems Engineering Research Center on Nanotechnology-Enabled Water Treatment, and the Lifecycle of Nanomaterials funded by US Environmental Protection Agency through the STAR program (RD83558001).

Compliance with ethical standards

Conflict of interest The authors declare that they have no conflict of interest.

References

Ambashta RD, Sillanpää M (2010) Water purification using magnetic assistance: a review. J Hazard Mater 180:38–49. https://doi.org/10.1016/j.jhazmat.2010.04.105

Deen WM (2011) Analysis of transport phenomena, 2nd edn. Oxford University Press

Gerber R (1978) Theory of particle capture in axial filters for high gradient magnetic separation. J Phys D Appl Phys 11:2119–2129. https://doi.org/10.1088/0022-3727/11/15/009

Gómez-Pastora J, Bringas E, Ortiz I (2014) Recent progress and future challenges on the use of high performance magnetic nano-adsorbents in environmental applications. Chem Eng J 256:187–204. https://doi.org/10.1016/j.cej.2014.06.119

Gutierrez AM, Dziubla TD, Hilt JZ (2017) Recent advances on iron oxide magnetic nanoparticles as sorbents of

organic pollutants in water and wastewater treatment. Rev Environ Health 32:111–117. https://doi.org/10.1515/reveh-2016-0063

Hatch GP, Stelter RE (2001) Magnetic design considerations for devices and particles used for biological high-gradient magnetic separation (HGMS) systems. J Magn Magn Mater 225: 262–276. https://doi.org/10.1016/S0304-8853(00)01250-6

Kikoin K, Drechsler S, Koepernik K et al (2015) Magnetic moment formation due to arsenic vacancies in LaFeAsO-derived superconductors. Sci Rep 5:1–11. https://doi.org/10.1038/srep11280

Larumbe S, Gómez-Polo C, Pérez-Landazábal JI, Pastor JM (2012) Effect of a SiO2 coating on the magnetic properties of Fe3O4 nanoparticles. J Phys Condens Matter 24:266007. https://doi.org/10.1088/0953-8984/24/26/266007

Mahmoudi M, Sant S, Wang B, Laurent S, Sen T (2011) Superparamagnetic iron oxide nanoparticles (SPIONs): development, surface modification and applications in chemotherapy. Adv Drug Deliv Rev 63:24–46. https://doi.org/10.1016/j.addr.2010.05.006

Mariani G, Fabbri M, Negrini F, Ribani PL (2010) High-gradient magnetic separation of pollutant from wastewaters using permanent magnets. Sep Purif Technol 72:147–155. https://doi.org/10.1016/j.seppur.2010.01.017

Moeser GD, Roach KA, Green WH et al (2004) High-gradient magnetic separation of coated magnetic nanoparticles. AICHE J 50:2835–2848. https://doi.org/10.1002/aic.10270

National Science Foundation (2013) NSF/ANSI 61 - 2013 drinking water system components - health effects. *http://www.nsf.org/newsroom_pdf/NSF_61-13_-_watermarked.pdf*

Oberteuffer J (1973) High gradient magnetic separation. Magn IEEE Trans 9:303–306. https://doi.org/10.1109/TMAG.1973.1067673

Oberteuffer J (1974) Magnetic separation: a review of principles, devices, and applications. Magn IEEE Trans 10:223–238. https://doi.org/10.1109/TMAG.1974.1058315

Qu X, Alvarez PJJ, Li Q (2013) Applications of nanotechnology in water and wastewater treatment. Water Res 47:3931–3946. https://doi.org/10.1016/j.watres.2012.09.058

Reza A, Mirrahimi MA (2010) Efficient separation of heavy metal cations by anchoring polyacrylic acid on superparamagnetic magnetite nanoparticles through surface modification. Chem Eng J 159:264–271. https://doi.org/10.1016/j.cej.2010.02.041

Ringler E, *Chatterton B*, *Philbrook D*, *Treatment MW* (2018) An advanced clarification process for treating produced waters. SPE prod Oper 154–163

Rossi LM, Costa NJS, Silva FP, Wojcieszak R (2014) Magnetic nanomaterials in catalysis: advanced catalysts for magnetic separation and beyond. Green Chem 16:2906. https://doi.org/10.1039/c4gc00164h

Tang T, *Liu F*, *Liu Y*, et al (2014) Identifying the magnetic properties of graphene oxide 123104:27–32. doi: https://doi.org/10.1063/1.4869827

Toh PY, Yeap SP, Kong LP et al (2012) Magnetophoretic removal of microalgae from fishpond water: feasibility of high gradient and low gradient magnetic separation. Chem Eng J 211–212:22–30. https://doi.org/10.1016/j.cej.2012.09.051

Veligatla M, Katakam S, Das S, Dahotre N, Gopalan R, Prabhu D, Arvindha Babu D, Choi-Yim H, Mukherjee S (2015) Effect of iron on the enhancement of magnetic properties for cobalt-based soft magnetic metallic glasses. Metall Mater Trans A 46:1019–1023. https://doi.org/10.1007/s11661-014-2714-2

Westerhoff P, Alvarez P, Gardea-Torresdey J et al (2016) Overcoming implementation barriers for nanotechnology in drinking water treatment. Environ Sci Nano 3:1241–1253. https://doi.org/10.1039/c6en00183a

Yavuz CT, Mayo JT, Suchecki C, Wang J, Ellsworth AZ, D'Couto H, Quevedo E, Prakash A, Gonzalez L, Nguyen C, Kelty C, Colvin VL (2010) Pollution magnet: Nano-magnetite for arsenic removal from drinking water. Environ Geochem Health 32:327–334. https://doi.org/10.1007/s10653-010-9293-y

Yavuz CT, Mayo JT, Yu WW et al (2006) Low-field magnetic separation of Monodisperse Fe3O4 Nanocrystals. Science 314(80):964–967. https://doi.org/10.1126/science.1131475

Zborowski M, Sun LP, Moore LR et al (1999) Continuous cell separation using novel magnetic quadrupole flow sorter. J Magn Magn Mater 194:224–230. https://doi.org/10.1016/S0304-8853(98)00581-2

Zhu Q, Ma J, Chen F et al (2019) Treatment of hydraulic fracturing flowback water using the combination of gel breaking , magnetic- enhanced coagulation , and electrocatalytic oxidation. Sep Sci Technol:1–8. https://doi.org/10.1080/01496395.2019.1614061